GEOLOGICA CARPATHICA, 2024, 75, 6, 405–414 https://doi.org/10.31577/GeolCarp.2024.21

Short communication

Apatite U–Pb dating of ultramafic lamprophyres (129 Ma) from the Klunst quarry (Germany): The oldest pre-rift magmatic event in the Saxo–Thuringian Zone

ADAM MAŤO[1,✉], LUKÁŠ KRMÍČEK[2,3], KLAUS P. STANEK[4] and JIŘÍ SLÁMA[2]

[1]Masaryk University, Faculty of Science, Department of Geological Sciences, Kotlářská 2, CZ-611 37 Brno, Czechia
[2]Institute of Geology of the Czech Academy of Sciences, Rozvojová 269, CZ-165 02 Prague, 6, Czechia
[3]Brno University of Technology, Faculty of Civil Engineering, Veveří 95, CZ-602 00 Brno, Czechia
[4]Freiberg University of Mining and Technology, Institute of Geology, D-09596 Freiberg, Germany

(Manuscript received August 20, 2024; accepted in revised form December 21, 2024; Associate Editor: Milan Kohút)

Abstract: This contribution presents a new laser ablation inductively-coupled plasma mass spectrometry (LA-ICP-MS) U–Pb age for magmatic apatite from ultramafic lamprophyres exposed in the Klunst quarry in Lusatia (south-eastern Saxony, Bohemian Massif). The lower intercept age of 129.3±2.2 Ma in the Tera-Wasserburg Concordia diagram confirms the previously published K/Ar and $^{40}Ar/^{39}Ar$ ages of phlogopite phenocrysts from similar ultramafic lamprophyres of the Klunst quarry. Therefore, it is possible to conclude that these ages indicate that the Klunst lamprophyres represent the oldest mantle-derived magmatic products related to incipient Alpine orogeny that affected the foreland of the Bohemian Massif.

Keywords: Bohemian Massif, Lusatia, U–Pb dating, ultramafic lamprophyres

Introduction

Lamprophyres represent mantle-derived (ultra)mafic and volatile-rich alkaline porphyritic rocks with euhedral to subhedral phenocrysts of primary OH-bearing mafic silicates. These include calcium amphibole and/or dark mica (biotite–phlogopite) along with felsic minerals that are confined to the groundmass (see Krmíček & Chalapathi Rao 2022 and references therein).

An extensive rift system formed in Western and Central Europe during the Alpine collision of the African and Eurasian plates in the Cenozoic (Prodehl et al. 2006; Ziegler et al. 2006). Volcanism associated with this system produced the large, circum-Mediterranean anorogenic Cenozoic igneous province documented by Lustrino & Wilson (2007). The most abundant anorogenic lithologies are Upper Cretaceous to Paleocene alkaline (Na-rich), mafic and ultramafic, locally melilitic igneous rocks, including various types of lamprophyres (e.g., Ulrych et al. 2022 and references therein).

The principal aim of our study is to verify the age of ultramafic lamprophyres collected at the Klunst quarry (Germany) within the Saxo–Thuringian Zone of the Bohemian Massif. Previously published studies (Renno et al. 2003a, b) indicate that these lamprophyres may represent a distinct and previously unknown Lower Cretaceous magmatic pulse from the CO_2-bearing mantle which occurred during the onset of the Alpine Orogeny.

The Lusatian Basement and dyke successions

The Lusatian block (Fig. 1) is a large unit of the Variscan orogen at the northern edge of the Bohemian Massif. It comprises multiple intrusions of Cadomian granodiorite emplaced into Neoproterozoic greywacke sequences (Linnemann et al. 2008). Cadomian magmatic activity ceased with intrusion of the late Cambrian Rumburk-type granite at 504±3 Ma (U–Pb zircon age; Zieger et al. 2018). During the Variscan orogeny, the Lusatian block was separated from the rising Erzgebirge metamorphic complex by a NW-trending strike-slip fault zone (WLF in Fig. 1), leaving the Lusatian block almost unaffected by subduction metamorphism or crustal stacking (Kroner & Romer 2013). However, it underwent numerous episodes of (ultra-)mafic to felsic magmatism (Abdelfadil et al. 2013; Käßner et al. 2021; Járóka et al. 2023). In the Upper Cretaceous, the Lusatian block was uplifted several kilometres along the Lusatian Thrust and the Lusatian Main Fault, and subsequently eroded (Käßner et al. 2020). This erosional and exhumation process exposed post-Cadomian magmatic pulses in the Lusatian block, thus providing a petrological window into mantle processes beneath the block during a significant period of time.

✉ corresponding author: Adam Mat'o
adam.matoo@gmail.com

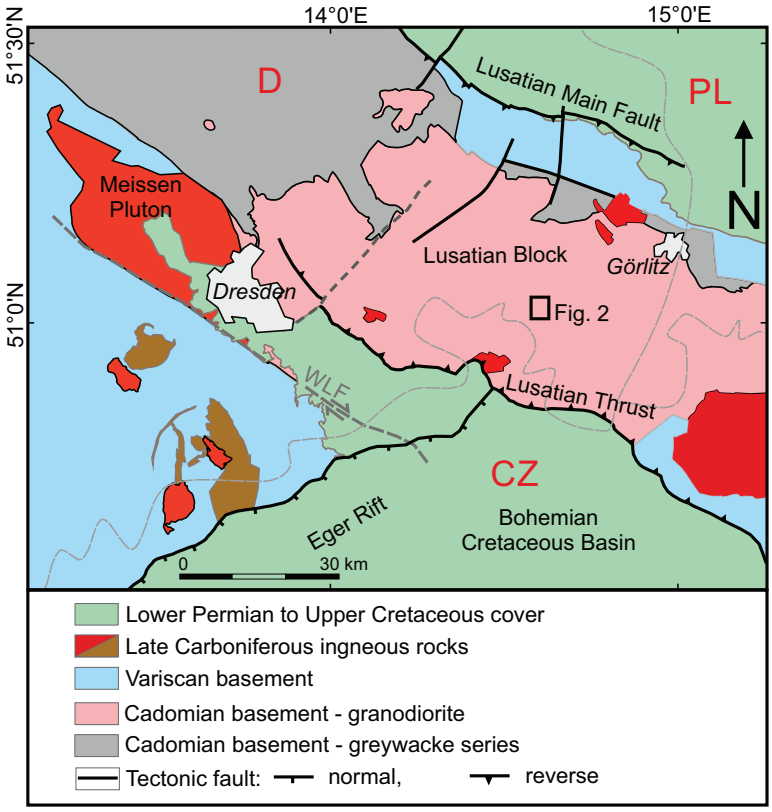

Fig. 1. Geological overview map of the Lusatian Block and surrounding geological units. WLF – Late Variscan dextral West-Lusatian fault system. Map simplified from Krentz et al. (2000).

The post-Cadomian igneous history comprises at least five magmatic intrusion stages of different age and composition (Kramer & Andrehs 2011). The oldest pulse comprises ~400 Ma (Middle to Upper Devonian) microgabbro stocks, sills, and dykes, as well as alkali doleritic and basaltic dykes that were emplaced during the early stages of the Variscan orogeny. Later, 325–335 Ma NE-trending spessartite dykes (amphibole and plagioclase dominant calc-alkaline lamprophyres) intruded the eastern part of the Lusatian block (Abdelfadil et al. 2013). The following felsic magmatic pulse formed late- to post-Variscan 300–315 Ma granite stocks, as well as dacitic to rhyolitic dykes (Käßner et al. 2021). The second youngest episode of magmatic activity in the Lusatian block is represented by 126 Ma dykes of ultramafic lamprophyres (Renno et al. 2003b). Magmatism within the Lusatian block ceased with emplacement of 27–35 Ma basanite to phonolite dykes and lavas, which are associated with syn-rift volcanism of the Eger rift (Büchner et al. 2015).

The presence of several hundred plugs and dykes of gabbro, diorite, and associated alkali basalt dykes, as well as spessartite dyke swarms, triggered a long-lasting discussion among petrologists on their classification and origin. This ongoing discussion is particularly focused on lamprophyres (see Kramer & Andrehs 2011, and citations therein; Abdelfadil et al. 2013). Ultramafic lamprophyre dykes, which are the focus of this study, are restricted to a small area near the town of Ebersbach (south-eastern Saxony, Germany).

The Klunst quarry

The Klunst quarry is located at the northern part of the town of Ebersbach within the Saxo–Thuringian Zone. Due to continuous and ongoing exploitation of granodiorite and microgabbro, the relationships between host basement rocks and the younger intrusions and dykes were exposed. The focus of this study is on the intrusions of lamprophyric rocks, which were first described by Lösch et al. (2000) and Renno et al. (2003a, b). Renno et al. (2003a) classified the lamprophyres as 'ultramafic alkaline lamprophyres' and determined their age range around 130–126 Ma (K/Ar on phlogopite: 130±5 Ma – Renno et al. 2003a; and $^{40}Ar/^{39}Ar$ on phlogopite: 126.64±0.27 Ma – Renno et al. 2003b). Renno et al (2003b) interpreted $^{40}Ar/^{39}Ar$ phlogopite age as the time of emplacement. Interestingly, similar rock types from the Bohemian Massif, which are related to pre-rift volcanic activity (*sensu* Ulrych et al. 2011), are ca. 50–60 Ma younger (e.g., Krüger et al. 2013; Ulrych et al. 2014, 2022).

The outcrops of ultramafic lamprophyre dykes studied by Renno et al. (2003a, b) had been completely weathered, and sample material adequate for petrographic and geochronological studies is no longer available. In this contribution, we study samples derived from new outcrops that have been exposed since then. We observed several basaltic dykes and multiple individual dykes, as well as a dyke swarm of ultramafic lamprophyre (UML) intruding the basement rocks. UML include sub-centimetre veinlets and dykes ranging in width up to several decimetres. Cross-cutting relationships indicate that the UML veins represent one of the youngest intrusions in the Klunst quarry. They intersect granodiorites, microgabbro, and a part of the basaltic dykes of the Lusatian block (Fig. 2). One noteworthy feature of UML is the number of macroscopic carbonate veinlets and nodules (Fig. 3) supporting a segregation event of silicate and carbonatitic melts, as proposed by Renno et al. (2003a).

Analytical methods

In total, 15 fresh samples were collected from the Klunst quarry in September 2022. The collected material was cut with a diamond saw, and a set of thin sections was made from the rock slices. Thin sections were used for optical microscopy for preliminary identification of mineral assemblages, as well

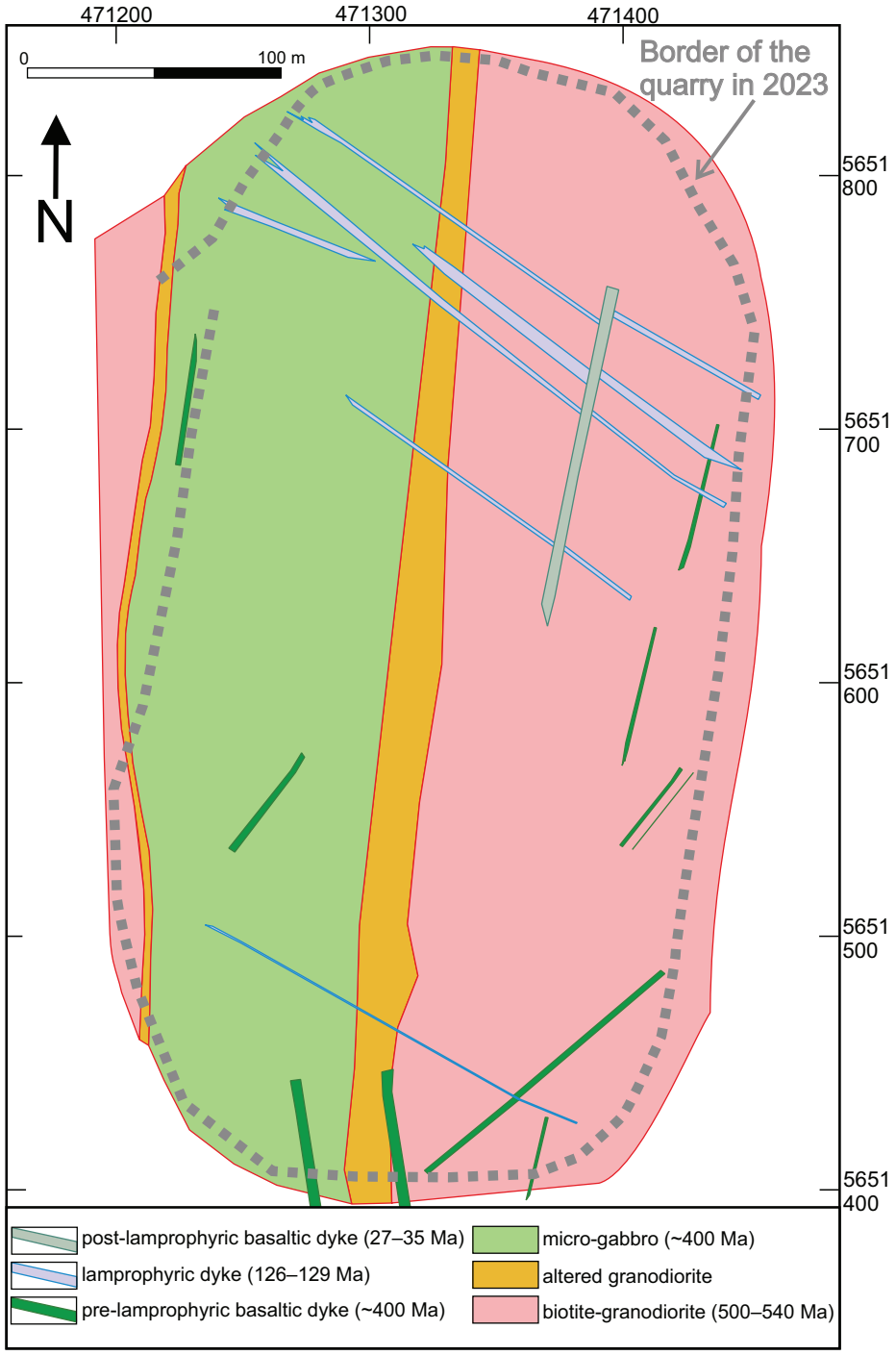

Fig. 2. Geological sketch of the Klunst quarry.

as for outlining points of interest for further chemical analyses. An Excel file (Table S1), with representative phlogopite, calcite, and apatite electron probe micro-analyser data is provided as Electronic Supplementary Material. One sample (KLN9) was selected for U–Pb dating using apatite.

A Thermo Scientific Element 2 sector field ICP-MS coupled to a 193 nm ArF excimer laser (Teledyne Cetac Analyte Excite laser) at the Institute of Geology of the Czech Academy of Sciences, Prague, Czech Republic, was used to measure the Pb/U and Pb isotopic ratios in apatite. The laser was fired at a repetition rate of 5 Hz and fluence of 5 J/cm^2 with a 50-micron spot size. The helium carrier gas was flushed through the two-volume ablation cell at a flow rate of 0.9 L/min and mixed with 0.7 L/min Ar and 0.006 L/min N prior to its introduction into the ICP. An in-house glass signal homogenizer (design by Tunheng & Hirata 2004) was used for mixing all the gases

Fig. 3. Carbonate veinlet in the central parts of an ultramafic lamprophyre dyke. An indication of segregation process during magma evolution.

and aerosol resulting in a smooth, spike-free signal. The signal was tuned for maximum sensitivity of Pb and U and low oxide level, commonly below 0.2 %. Typical acquisitions consisted of 15 seconds of blank measurement followed by measurement of U, Th, and Pb signals from the ablated apatite for another 37 seconds. A total of 385 mass scans data were acquired in time resolved – peak jumping – pulse counting/analogue mode with 1 point measured per peak for masses (dwell time) ^{202}Hg (10 ms), ^{204}Pb+Hg (10 ms), ^{206}Pb (15 ms), ^{207}Pb (30 ms), ^{208}Pb (10 ms), ^{232}Th (10 ms), ^{235}U (20 ms), and ^{238}U (10 ms). Due to a non-linear transition between the counting and analogue acquisition modes of the ICP instrument, and the fact that ^{238}U is usually measured in "both" modes, the raw data were pre-processed using a Python routine for decoding the Thermo Element ICPMS data files (Hartman et al. 2017) and an in-house Excel macro. As a result, the intensities of ^{238}U were left unchanged if measured in a counting mode and recalculated from ^{235}U intensities, if the ^{238}U was acquired in analogue mode. Data reduction was carried out off-line using a modified version of the VizualAge U–Pb data reduction package for Iolite 3.5 (VizualAge_UcomPbine) following the method described by Chew et al. (2014). Data reduction included correction for gas blank, laser-induced elemental fractionation of Pb and U, and instrument mass bias using the ^{207}Pb method for common Pb correction of apatite age reference material. For the data presented here, blank intensities and instrumental bias were interpolated using an automatic spline function while down-hole inter-element fractionation was corrected using an exponential function. The method is based on a session-wide, downhole fractionation model obtained from the measured apatite reference material with variable Pbc/Pbrad. This type of model is then applied to other analysed data using sample-standard bracketing. For the presented data, the Madagascar apatite reference material (473.5 Ma) of Chew et al. (2014) was used as primary standard. Durango (31.44±0.18 Ma; McDowell et al. 2005) and McClure (523.5±2 Ma; Schoene & Bowring 2006) apatites were periodically analysed during the measurement for quality control. The obtained U–Pb Concordia intercept age of 522±16 Ma (MSWD=2.2; n=10) from McClure and 31.1±2.6 Ma (MSWD=0.57; n=10) from Durango apatite correspond well with the reference values. The larger error on the secondary materials is caused by the limited number of analysed spots for each standard.

The apatite age is presented as a U–Pb Concordia intercept age generated with the ISOPLOT program v. 4.16 (Ludwig 2008).

Petrography and mineralogy

Some of the rock samples are macroscopically more homogenous than typical lamprophyres (Rosenbusch 1887; Krmíček & Chalapathi Rao 2022 and references therein). Phenocrysts of phlogopite are still visible in a dark, fine-grained matrix, and the characteristic lamprophyre lustre is obvious on fresh cuts. Their colours range from medium grey (N5; Munsell colour system) to medium dark grey (N4). A brown tint is common on mildly weathered surfaces and on contacts with host rocks. A few samples contained carbonate veinlets and nodules. Carbonate nests reach up to several centimetres in size.

In thin sections, the *phlogopite* occurs as several millimetres-long phenocrysts or as small groundmass grains. Unlike these two mentioned forms, which tend to be euhedral to subhedral, there is a third, little less common, form that is specifically anhedral – a poikilitic (madupitic-like) phlogopite filling up the space between other matrix minerals, as well as enclosing several of them (cf. Mitchell & Bergman 1991). Euhedral to subhedral phenocrysts and groundmass grains show signs of deformation — predominantly various degrees of bending, apparent recrystallization of edges, and sometimes parting along cleavage planes. Back-scattered electron (BSE) imaging revealed frequent zoning (see Fig. S1 and Table S1 in Electronic Supplementary Material). In several samples, zoning in the marginal parts corresponds to the green edges that have been previously observed in numerous phlogopite grains during microscopy in polarized light. Gradual, smooth transitions from 'normal' brown phlogopite to such green phases led us to suspect that the margins may represent a *yangzhumingite* phase, rather than the result of chloritization (Kullerud et al. 2011; Miyawaki et al. 2011; Schingaro et al. 2014). This rare mineral has only been observed in contacts between phlogopite and calcite.

Pyroxenes are another important constituent of the samples; they are mainly present as clinopyroxenes. In the majority of samples, clinopyroxene is the second most common mafic

mineral after phlogopite. *Amphibole* relicts are extremely rare. Similarly, *olivine* is almost exclusively present as pseudomorphs and relicts. Even then, its occurrence is rare.

Another abundantly present mineral group are *carbonates*. With serpentine minerals and talc (±chlorite), they make up plentiful relicts and pseudomorphs of pyroxenes, olivines, and amphiboles. However, in line with the earlier study of Renno et al. (2003a, b), we assume that groundmass carbonate, which is mostly calcite, is of magmatic origin. Several calcite grains intergrown with phlogopite and apatite were observed. In addition to that, we consider the phlogopite margins to be evidence of a liquid to subsolid stage interaction with calcite (see Fig. S1 in Electronic Supplementary Material).

Contrary to carbonates, *melilite*, which is considered a defining characteristic of ultramafic lamprophyres of the polzenite or alnöite-type, has not yet been observed. *Apatite* is common and is one of the most abundant accessory minerals. It is present as small anhedral groundmass grains, and also as larger subhedral needles (up to 2 mm in length) or short-column shaped grains.

From the opaque minerals, we have quantitatively confirmed the presence of *magnetite* and *ilmenite*. They occur predominantly as irregular specks in between, or 'on top of', phenocrysts and matrix minerals.

Apatite U–Pb dating

A total of 42 apatite grains (larger needles) were dated using the LA-ICP-MS U–Pb dating method (Table 1; see also Table S2 in the Electronic Supplement) resulting in a 129.3±2.2 Ma age as shown on Tera-Wasserburg Concordia (Fig. 4). This overlaps with the $^{40}Ar/^{39}Ar$ step-heating age for magmatic phlogopite presented by Renno et al. (2003b) and confirms that the ultramafic lamprophyres from the Klunst quarry belong to a separate mantle-related magmatic event that preceded the main periods of volcanic activity, which accompanied the rifting processes that created the Ohře (Eger) rift of the Bohemian Massif (rift-related volcanic activity *sensu* Ulrych et al. 2011). We interpret the resulting age in accordance with Renno et al. (2003b) as the time of ascent and emplacement of the ultramafic lamprophyres.

Discussion

The age presented by Renno et al. (2003b) that was acquired by the $^{40}Ar/^{39}Ar$ stepwise heating technique on phlogopite, with a weighted mean plateau age of 126.64±0.27 Ma, seemed a bit unusual in the wider scope. Looking at the broader area of the Saxo–Thuringian Zone, similar rocks from the Osečná and Delitzsch complexes are much younger, in fact, approximately half the age of the Klunst UML. Ultramafic melilitic rocks from Osečná are within the range of 68–59 Ma (K/Ar; Pivec et al. 1998; Ulrych et al. 2022 and references therein). The latest dating results of the Delitzsch Complex provided the 73–72 Ma Rb–Sr phlogopite and U–Pb baddeleyite ages for ultramafic lamprophyres and carbonatites respectively (Krüger et al. 2013). These Upper Cretaceous to Paleocene ages place the Osečná and Delitzsch complex into the pre-rift period of volcanic activity in the Bohemian Massif according to Ulrych et al. (2011). In this light, the age of the Klunst UML appeared to be a geological anomaly. We decided to test Renno et al. (2003b) age, assuming its theoretical inaccuracy to be potentially caused by the presence of phlogopite xenocrysts and using a fundamentally different dating technique.

Renno et al. (2003a) provided a petrogenetic model which suggested that the magmatic evolution of the Klunst UML was triggered by a mantle plume reaching the garnet–lherzolitic mantle. The model accounts for metasomatic enrichment of the mantle by carbonatitic melts. Renno et al. (2003a) relied on evidence for this kind of process found by Seifert & Thomas (1995) and Frýda & Vokurka (1995) in wehrlite xenoliths from tertiary tephrite of the Grosser Winterberg (Saxon Switzerland, Eastern Germany). At the stage of this metasomatic enrichment, a primary alkaline basaltic melt had been generated. In a strongly-carbonatized lithospheric mantle, a rising mantle plume led to the formation of melts highly enriched in incompatible elements. These melts reached the crust very rapidly and formed the alkaline ultramafic lamprophyric and a small amount of carbonatitic melts through segregation processes (Renno et al. 2003a).

According to Voigt (2009), a sedimentary basin on top of the Lusatian Fault was transformed into a graben structure during the Lower Cretaceous and was later uplifted (Käßner et al. 2020). Such an event would correlate with our limited field observations, in that the UML seemed to fill extensional fractures in Cadomian granodiorites. Based on the dating by Renno et al. (2003b), Käßner et al. (2020) also consider the UML as an indicator for extensional tectonics during this period.

Ostendorf et al. (2019) investigated polymetallic mineralization in the Freiberg mining district and identified three types of veins, which they assigned to two separate stages of mineralization. The first two veining types representing the first stage are of the quartz-bearing polymetallic sulfide type and the carbonate-bearing polymetallic sulfide type. The third vein type attributed to the second stage is of the barite–fluorite–sulfide type. Dating these mineralization stages by the Rb–Sr mineral isochron method yielded an early Permian age of 276±16 Ma for the first stage, and a Cretaceous age of 121.3±4.2 Ma for the second stage. The dating of this mineralization stage is very close to the ages reported for the Klunst UML and the similar ages could reflect a related post-magmatic hydrothermal event. Ostendorf et al. (2019) attributed the F–Ba mineralization to fluid circulation related to an extensional event during the early opening of the North Atlantic Ocean.

The results presented in this contribution (Fig. 4, Table 1; Table S2 in the Electronic Supplement), along with the results of Renno et al. (2003a, b), provide robust evidence that ultramafic lamprophyres from the Klunst quarry are indeed much

Table 1: Apatite isotopic and age data. §disc. – discordance was calculated as (1−((AGE $^{206}Pb/^{238}U$)/ (AGE $^{207}Pb/^{206}Pb$)))*100.

	Ratios							Ages						
Analysis	$^{206}Pb/^{204}Pb$	$^{207}Pb/^{235}U$	±2σ	$^{206}Pb/^{238}U$	±2σ	$^{207}Pb/^{206}Pb$	±2σ	$^{207}Pb/^{235}U$ age	±2σ	$^{206}Pb/^{238}U$ age	±2σ	$^{207}Pb/^{206}Pb$ age	±2σ	§disc
1	4	6.000	0.350	0.074	0.004	0.5640	0.0130	461	27	1905	62	34	18	−5553
3	6	1.246	0.035	0.030	0.001	0.2952	0.0054	194	8	819	16	48	13	−1606
4	6	1.446	0.042	0.032	0.001	0.3231	0.0065	206	9	905	17	43	13	−2005
5	5	1.345	0.039	0.032	0.001	0.3061	0.0062	201	9	862	17	24	7	−3492
8	6	1.588	0.044	0.034	0.002	0.3445	0.0067	213	9	965	18	24	8	−3921
9	4	6.330	0.580	0.078	0.006	0.5450	0.0170	481	36	1881	72	11	7	−16546
10	4	11.740	0.320	0.127	0.006	0.6720	0.0140	770	33	2578	26	17	11	−15524
12	5	1.800	0.062	0.036	0.002	0.3644	0.0077	228	10	1041	22	27	9	−3756
13	5	1.307	0.050	0.031	0.001	0.3002	0.0061	199	9	838	17	32	10	−2519
15	5	1.135	0.034	0.030	0.001	0.2758	0.0057	190	8	768	16	47	13	−1534
16	6	1.162	0.047	0.029	0.001	0.2876	0.0076	186	8	773	17	27	9	−2763
18	6	0.964	0.029	0.028	0.001	0.2534	0.0056	176	8	683	15	33	7	−1970
19	6	1.052	0.029	0.028	0.001	0.2692	0.0052	181	8	728	14	55	15	−1224
20	3	1.530	0.067	0.034	0.002	0.3293	0.0097	213	10	930	26	13	5	−6945
21	4	1.111	0.034	0.030	0.001	0.2726	0.0056	188	8	755	16	27	7	−2696
23	5	8.500	1.100	0.099	0.011	0.6080	0.0150	592	59	2113	69	18	12	−11639
24	6	1.670	0.074	0.034	0.002	0.3440	0.0087	218	10	980	27	22	8	−4355
26	5	1.045	0.034	0.029	0.001	0.2626	0.0068	183	8	723	17	53	12	−1264
27	4	1.215	0.038	0.030	0.001	0.2928	0.0063	189	8	804	17	32	5	−2413
28	3	6.910	0.200	0.082	0.004	0.6120	0.0130	508	22	2095	25	15	9	−13867
29	7	1.424	0.040	0.032	0.001	0.3196	0.0058	204	9	898	17	20	7	−4390
30	5	2.856	0.100	0.047	0.002	0.4380	0.0100	295	13	1359	26	14	7	−9607
31	3	1.483	0.071	0.034	0.002	0.3210	0.0110	212	10	906	29	−7	−3	13424
32	7	1.159	0.032	0.030	0.001	0.2778	0.0052	192	8	779	15	8	−1	−9641
33	4	1.035	0.030	0.029	0.001	0.2598	0.0052	184	8	719	15	5	3	−14286
34	4	1.215	0.040	0.030	0.001	0.2946	0.0064	193	8	802	18	30	7	−2573
35	5	1.715	0.057	0.035	0.002	0.3595	0.0083	221	10	1009	22	−4	−1	25325
39	9	1.128	0.032	0.030	0.001	0.2753	0.0058	189	8	764	15	−33	−5	2415
40	6	1.252	0.038	0.030	0.001	0.2993	0.0062	193	8	822	17	27	7	−2944
41	8	1.208	0.038	0.031	0.001	0.2868	0.0069	195	9	800	18	−52	−11	1638
42	6	1.137	0.033	0.030	0.001	0.2732	0.0058	192	8	769	16	−4	−1	19325
44	5	1.340	0.039	0.032	0.001	0.3076	0.0053	200	9	860	17	23	8	−3639
45	6	1.451	0.044	0.032	0.001	0.3300	0.0066	203	9	906	18	30	10	−2920
46	5	1.590	0.120	0.034	0.002	0.3230	0.0110	217	11	922	36	48	13	−1821
47	4	1.100	0.064	0.029	0.002	0.2690	0.0100	185	9	734	31	17	4	−4218
48	6	1.726	0.053	0.035	0.002	0.3619	0.0084	221	10	1017	20	9	4	−11200
49	3	1.200	0.036	0.030	0.001	0.2882	0.0061	191	8	798	17	35	10	−2180
52	4	5.700	0.170	0.070	0.003	0.5930	0.0150	436	19	1930	26	14	7	−14091
53	5	1.093	0.030	0.029	0.001	0.2741	0.0048	184	8	748	15	54	15	−1285
54	5	1.756	0.077	0.035	0.002	0.3660	0.0110	219	10	1021	28	30	11	−3303
55	7	1.447	0.041	0.033	0.002	0.3177	0.0055	209	9	906	17	26	9	−3385
56	4	1.096	0.034	0.030	0.001	0.2637	0.0059	191	9	750	16	19	5	−3847

Table 1 (continued)

	Ratios							Ages						
Analysis	**$^{206}Pb/^{204}Pb$**	**$^{207}Pb/^{235}U$**	**±2σ**	**$^{206}Pb/^{238}U$**	**±2σ**	**$^{207}Pb/^{206}Pb$**	**±2σ**	**$^{207}Pb/^{235}U$ age**	**±2σ**	**$^{206}Pb/^{238}U$ age**	**±2σ**	**$^{207}Pb/^{206}Pb$ age**	**±2σ**	**§disc**
Reference materials data:														
Durango	1	0.129	0.009	0.006	0.000	0.169	0.013	38	2	122	8	3	0	−224
	1	0.213	0.013	0.007	0.000	0.239	0.015	43	2	194	11	−2	0	−356
	0	0.158	0.010	0.006	0.000	0.198	0.014	38	2	147	9	4	1	−287
	0	0.179	0.015	0.006	0.000	0.225	0.018	39	2	160	11	2	1	−312
	1	0.176	0.014	0.006	0.000	0.216	0.017	40	2	162	11	5	1	−307
	0	0.153	0.010	0.006	0.000	0.194	0.012	38	2	142	9	1	0	−278
	1	0.137	0.009	0.006	0.000	0.174	0.012	38	2	129	8	7	1	−240
	1	0.178	0.013	0.006	0.000	0.221	0.018	41	2	161	10	6	1	−296
	0	0.193	0.015	0.006	0.000	0.237	0.018	41	2	176	12	3	0	−329
	0	0.221	0.018	0.007	0.000	0.251	0.018	42	3	196	13	0	0	−364
Madagascar	2	0.580	0.024	0.074	0.003	0.056	0.002	462	19	459	15	33	3	1
	2	0.592	0.048	0.076	0.003	0.056	0.004	473	20	449	30	45	3	5
	2	0.595	0.024	0.076	0.003	0.057	0.002	473	19	470	15	38	3	1
	2	0.591	0.024	0.076	0.003	0.056	0.002	475	19	470	16	100	5	1
	5	0.614	0.025	0.078	0.003	0.057	0.002	485	20	482	15	114	9	1
	2	0.585	0.042	0.075	0.003	0.056	0.004	465	19	451	26	85	4	3
	2	0.578	0.022	0.074	0.003	0.057	0.002	462	19	459	14	9	1	1
	2	0.612	0.045	0.079	0.003	0.057	0.004	488	20	462	29	69	4	5
	2	0.601	0.024	0.077	0.003	0.057	0.002	477	20	475	15	131	5	1
	2	0.594	0.023	0.076	0.003	0.057	0.002	474	20	469	14	93	4	1
McClure	2	4.050	0.140	0.116	0.005	0.257	0.006	706	30	1638	27	35	9	−4527
	5	2.964	0.095	0.104	0.005	0.205	0.005	639	27	1394	24	42	9	−3219
	3	3.628	0.110	0.113	0.005	0.232	0.005	692	28	1549	25	26	7	−5858
	11	4.240	0.170	0.118	0.006	0.260	0.010	721	33	1676	33	81	20	−1969
	11	2.476	0.083	0.101	0.005	0.178	0.005	619	28	1261	24	128	24	−885
	2	4.411	0.140	0.119	0.005	0.270	0.006	726	30	1712	26	6	3	−26650
	4	2.210	0.077	0.098	0.004	0.162	0.004	604	26	1180	24	49	9	−2308
	5	3.353	0.120	0.111	0.005	0.217	0.005	678	28	1488	28	44	11	−3282
	4	2.559	0.078	0.104	0.005	0.178	0.005	636	27	1285	23	20	4	−6325

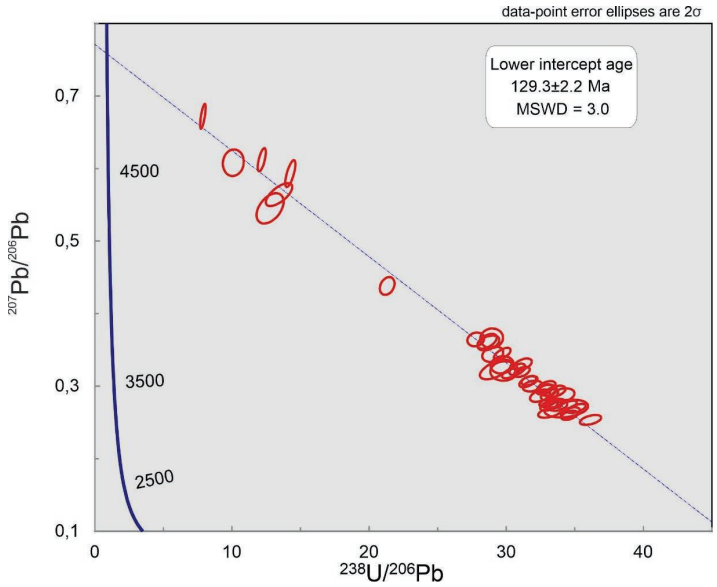

Fig. 4. Tera-Wasserburg Concordia diagram for apatite grains separated from sample KLN9.

older than similar rocks in the Saxo–Thuringian Zone. Taking into account previously published interpretations of the regional geological evolution, we interpret the Klunst UML as the first (oldest) magmatic indicators of the Alpine orogeny affecting the Bohemian Massif. Alternatively, and more broadly, as evidence for changes in relative movements and collisions between Africa, Europe, and Iberia (Ziegler 1987; Dèzes et al. 2004; Ziegler et al. 2006; Kley & Voigt 2008). Considering the significant difference in the ages of the Klunst lamprophyres and similar rocks from the Osečná and Delitzsch complexes, we conclude that the Klunst UML belong to a separate magmatic event. However, this conclusion does not necessarily disregard the potential connection of the Klunst lamprophyres to the pre-rift period of volcanic activity in the Bohemian Massif (*sensu* Ulrych et al. 2011) and to the events that accompanied the opening of the Eger rift. The existence of a mantle plume (Wilson & Downes 1991) or a mantle hot finger (model of Granet et al. 1995; Wilson & Patterson 2001; Lustrino & Wilson 2007) underlying the Central European Volcanic Province remains debatable (Ulrych et al. 2011 and references therein). Rather than mantle plume activity, lithospheric extension, and uplift described by several authors as summarized in Käßner et al. (2020) may just as well have been triggered by passive diapiric upwelling of partially melted upper mantle material.

Conclusions

We have verified and confirmed the results presented by Renno et al. (2003b) by in situ U–Pb dating of magmatic apatite yielding an age of 129.3±2.2 Ma. Our results overlap with the reported K/Ar and $^{40}Ar/^{39}Ar$ phlogopite ages. Furthermore, our age and those reported by Renno et al. (2003a, b) correlate with an extensional event (Voigt 2009). Our results challenge the assumption that the Klunst lamprophyres could be related to the same magmatic event as either the more widespread Upper Cretaceous–Paleocene ultramafic lamprophyres of polzenite type in the Osečná Complex, or the Upper Cretaceous alnöites and carbonatites from the Delitzsch Complex. Thus, we conclude that the Klunst ultramafic lamprophyres represent, as of yet, an isolated mantle-related magmatic pulse. We interpret the Klunst UML intrusions as the first, initial, magmatic indicators of the Alpine orogeny affecting the Bohemian Massif.

Acknowledgements: This research was financially supported by the RVO 67985831 project of the Institute of Geology of the Czech Academy of Sciences, the grant No. FAST-S-24-8658 to Brno University of Technology, and the EXPRO 2019 project of the Czech Science Foundation (No. 19-29124X) to LK. We are indebted to Daniel Müller (Las Condes, Santiago, Chile) for his valuable advice and recommendations on the first draft of the manuscript. We thank Martin J. Timmerman (University of Potsdam, Germany) and David Chew (Trinity College Dublin, Ireland) and two anonymous reviewers, who all significantly helped improve the quality of the manuscript, as well as to associate editor Milan Kohút for smooth editorial handling.

References

Abdelfadil K.M., Romer R.L., Seifert T. & Lobst R. 2013: Calc-alkaline lamprophyres from Lusatia (Germany) – Evidence for a repeatedly enriched mantle source. *Chemical Geology* 353, 230–245. https://doi.org/10.1016/j.chemgeo.2012.10.023

Büchner J., Tietz O., Viereck L., Suhr P. & Abratis M. 2015: Volcanology, geochemistry and age of the Lausitz Volcanic Field. *International Journal of Earth Sciences* 104, 2057–2083. https://doi.org/10.1007/s00531-015-1165-3

Chew D.M., Petrus J.A. & Kamber B.S. 2014: U–Pb LA-ICPMS dating using accessory mineral standards with variable common Pb. *Chemical Geology* 363, 185–199. https://doi.org/10.1016/j.chemgeo.2013.11.006

Dèzes P., Schmid S.M. and Ziegler P.A. 2004: Evolution of the European Cenozoic Rift System: interaction of the Alpine and Pyrenean orogens with their foreland lithosphere. *Tectonophysics* 389, 1–33. https://doi.org/10.1016/j.tecto.2004.06.011

Frýda J. & Vokurka K. 1995: Evidence for carbonatite metasomatism in the upper mantle beneath the Bohemian Massif. *Journal of the Czech Geological Society* 43, A-9-10.

Granet M., Wilson M. & Achauer U. 1995: Imaging mantle plumes beneath the French Massif Central. *Earth and Planetary Science Letters* 136, 199–203. https://doi.org/10.1016/0012-821X(95)00174-B

Hartman J., Franks R., Gehrels G., Hourigan J. & Wenig P. 2017: Decoding data files from a Thermo ElementTM ICP Mass Spectrometer. 1–15, manual available online at https://github.com/jhh67/extractdat.git

Járóka T., Pfänder J.A., Seifert T., Hauff F., Sperner B., Staude S. & Schulz B. 2023: Age and petrogenesis of Ni–Cu–(PGE) sulfide-bearing gabbroic intrusions in the Lausitz Block, northern Bohemian Massif (Germany/Czech Republic). *Lithos* 444–445, 107090. https://doi.org/10.1016/j.lithos.2023.107090

Käßner A., Stanek K.P. & Lapp M. 2020: Post-Variscan tectonic and landscape evolution of the Elbe Fault Zone and the Lusatian Block based on apatite fission-track data and geomorphologic constraints. *Geomorphology* 355, 106860. https://doi.org/10.1016/j.geomorph.2019.106860

Käßner A., Tichomirowa M., Lapp M., Leonhardt D., Whitehouse M. & Gerdes A. 2021: Two-phase late Paleozoic magmatism (~313–312 and ~299–298 Ma) in the Lusatian Block and its relation to large scale NW striking fault zones: evidence from zircon U–Pb CA–ID–TIMS geochronology, bulk rock-and zircon chemistry. *International Journal of Earth Sciences* 110, 2923–2953. https://doi.org/10.1007/s00531-021-02092-y

Kley J. & Voigt T. 2008: Late Cretaceous intraplate thrusting in central Europe: effect of Africa-Iberia Europe convergence, not Alpine collision. *Geology* 36, 839–842. https://doi.org/10.1130/G24930A.1

Kramer W. & Andrehs G. 2011: Basische Gangintrusionen im Oberlausitzer Bergland, Ostsachsen. *Berichte der Naturforschenden Gesellschaft der Oberlausitz* 19, 21–46.

Krentz O., Walter H., Brause H., Hoth K., Kozdrój W., Cymerman Z., Opletal M. & Mrázová S. 2000: Geological Map Lausitz–Jizera–Karkonosze (without Cenozoic sediments), 1:100,000.

Krmíček L. & Chalapathi Rao N.V. 2022: Lamprophyres, lamproites and related rocks as tracers to supercontinent cycles and metallogenesis. *The Geological Society of London* 513, 1–16. https://doi.org/10.1144/SP513-2021-159

Kroner U. & Romer R.L. 2013: Two plates – Many subduction zones: The Variscan orogeny reconsidered. *Gondwana Research* 24, 298–329. https://doi.org/10.1016/j.gr.2013.03.001

Krüger J.C., Romer R.L. & Kämpf H. 2013: Late Cretaceous ultramafic lamprophyres and carbonatites from the Delitzsch Complex, Germany. *Chemical Geology* 353, 140–150. https://doi.org/10.1016/j.chemgeo.2012.09.026

Kullerud K., Zozulya D., Bergh S.G., Hansen H. & Ravna E.J.K. 2011: Geochemistry and tectonic setting of a lamproite dyke in Kvaløya, North Norway. *Lithos* 126, 278–289. https://doi.org/10.1016/j.lithos.2011.08.002

Linnemann U., Romer R.L., Pin C., Aleksandrowski P., Buła Z., Geisler T., Kachlik V., Krzemińska E., Mazur S., Motuza G., Murphy J.B., Nance R.D., Pisarevsky S.A., Schulz B., Ulrich J., Wiszniewska J., Żaba J. & Zeh A. 2008: Precambrian. In: McCann T. (Ed.): The Geology of Central Europe, Volume 1 – Precambrian and Palaeozoic. *The Geological Society of London*, 21–101. https://doi.org/10.1144/cev1p.2

Lösch C., Renno A.D., Stanek K.P. & Lobst R. 2000: Petrology of Late Cretaceous ultramafic lamprophyres in the Lausitz-Massiv (Germany). *Berichte der Deutschen Mineralogischen Gesellschaft, Beiheft European Journal of Mineralogy* 12, 115.

Ludwig K.R. 2008: Isoplot 3.70. A geochronological toolkit for Microsoft Excel. *Berkley Geochronology Center Special Publication* No. 4, 76.

Lustrino M. & Wilson M. 2007: The circum-Mediterranean anorogenic Cenozoic igneous province. *Earth-Science Review* 81, 1–65. https://doi.org/10.1016/j.earscirev.2006.09.002

McDowell F.W., McIntosh W.C. & Farley K.A. 2005: A precise ^{40}Ar–^{39}Ar reference age for the Durango apatite (U–Th)/He and fission-track dating standard. *Chemical Geology* 214, 249–263. https://doi.org/10.1016/j.chemgeo.2004.10.002

Mitchell R.H. & Bergman S.C. 1991: Petrology of Lamproites. *Plenum Press*, New York. https://doi.org/10.1007/978-1-4615-3788-5

Miyawaki R., Shimazaki H., Shigeoka M., Yokoyama K., Matsubara S. & Yurimoto H. 2011: Yangzhumingite, $KMg_{2.5}Si_4O_{10}F_2$, a new mineral in the mica group from Bayan Obo, Inner Mongolia. *European Journal of Mineralogy* 23, 467–473. https://doi.org/10.1127/0935-1221/2011/0023-2098

Ostendorf J., Henjes-Kunst F., Seifert T. & Gutzmer J. 2019: Age and genesis of polymetallic veins in the Freiberg district, Erzgebirge, Germany: constraints from radiogenic isotopes. *Mineralium Deposita* 54, 217–236, https://doi.org/10.1007/s00126-018-0841-1

Pivec E., Ulrych J., Höhndorf A. & Rutšek J. 1998: Melilitic rocks from northern Bohemia: geochemistry and mineralogy. *Neues Jahrbuch für Mineralogie – Abhandlungen Journal of Mineralogy and Geochemistry* 173, 119–154. https://doi.org/10.1127/njma/173/1998/119

Prodehl C., Mueller St. & Haak V. 2006: The european cenozoic rift system. In: Olsen K.H. (Ed.): Continental rifts: evolution, structure, tectonics. *Developments in Geotectonics* 25, 133–212. https://doi.org/10.1016/S0419-0254(06)80012-1

Renno A.D., Stanek K.P., Lobst R & Pushkarev Y. 2003a: A new lamprophyre species from the Klunst quarry (Ebersbach, Lusatia, Germany) – geochemical and petrological implications. *Zeitschrift für Geologische Wissenschaften* 31, 1–20.

Renno A.D., Hacker B.R. & Stanek K.P. 2003b: An Early Cretaceous (126 Ma) ultramafic alkaline lamprophyre from the quarry Klunst (Ebersbach, Lusatia, Germany). *Zeitschrift für Geologische Wissenschaften* 31, 31–36.

Rosenbusch H. 1887: Mikroskopische Physiographie der Mineralien und Gesteine. Band II: Massige Gesteine. *E. Schweizerbart'sche Verlagsbuchhandlung*, Stuttgart.

Seifert W. & Thomas R. 1995: Silicate-carbonate Immiscibility: A Melt Inclusion Study of Olivine Melilitite and Wehrlite Xenoliths im Tephrite from the Elbe Zone, Germany. *Chemie der Erde* 55, 263–279.

Schingaro E., Kullerud K., Lacalamita M., Mesto E., Scordari F., Zozulya D., Erambert M. & Ravna E.J.K. 2014: Yangzhumingite and phlogopite from the Kvaløya lamproite (North Norway): Structure, composition and origin. *Lithos* 210–211, 1–13. https://doi.org/10.1016/j.lithos.2014.09.020

Schoene B. & Bowring S.A. 2006: U–Pb systematics of the McClure Mountain syenite: thermochronological constraints on the age of the ^{40}Ar/^{39}Ar standard MMhb. *Contributions to Mineralogy and Petrology* 151, 615–630. https://doi.org/10.1007/s00410-006-0077-4

Tunheng A. & Hirata T. 2004: Development of signal smoothing device for precise elemental analysis using laser ablation-ICP-mass spectrometry. *Journal of Analytical Atomic Spectrometry* 19, 932. https://doi.org/10.1039/B402493A

Ulrych J., Dostal J., Adamovič J., Jelínek E., Špaček P., Hegner E. & Balogh K. 2011: Recurrent Cenozoic volcanic activity in the Bohemian Massif (Czech Republic). *Lithos* 123, 133–144. https://doi.org/10.1016/j.lithos.2010.12.008

Ulrych J., Adamovič J., Krmíček L., Ackerman L. & Balogh K. 2014: Revision of Scheumann's classification of melilitic lamprophyres and related melilitic rocks in light of new analytical data. *Journal of Geosciences* 59, 47–66. https://doi.org/10.3190/jgeosci.158

Ulrych J., Krmíček L., Adamovič J. & Krmíčková S. 2022: The story of post-Variscan lamprophyres of the Bohemian Massif: from ultramafic (Upper Cretaceous–Paleocene) to alkaline (Eocene–Oligocene) types. *The Geological Society of London, Special Publications* 513, 237–269. https://doi.org/10.1144/SP513-2020-233

Voigt T. 2009: Die Lausitz-Riesengebirgs-Antiklinalzone als kreidezeitliche Inversionsstruktur: Geologische Hinweise aus den umgebenden Kreidebecken. *Zeitschrift für geologische Wissenschaften* 37, 15–39.

Wilson M. & Downes H. 1991: Tertiary–Quaternary extension-related alkaline magmatism in western and central Europe. *Journal of Petrology* 32, 811–850. https://doi.org/10.1093/petrology/32.4.811

Wilson M. & Patterson R. 2001: Intraplate magmatism related to short-wavelength convective instabilities in the upper mantle: Evidence from the Tertiary–Quaternary volcanic province of western and central Europe. In: Ernst R.E. & Buchan K.L. (Eds.): Mantle Plumes: Their Identification Through Time. *Geological Society of America Special Paper* 352, 37–58. https://doi.org/10.1130/0-8137-2352-3.37

Zieger J., Linnemann U., Hofmann M., Gärtner A., Marko L. & Gerdes A. 2018: A new U–Pb LA-ICP-MS age of the Rumburk granite (Lausitz Block, Saxo–Thuringian Zone): constraints for a magmatic event in the Upper Cambrian. *International Journal of Earth Sciences* 107, 933–953. https://doi.org/10.1007/s00531-017-1511-8

Ziegler P.A. 1987: Late Cretaceous and Cenozoic intraplate compressional deformations in the Alpine Foreland – a geodynamic model. *Tectonophysics* 137, 389–420. https://doi.org/10.1016/0040-1951(87)90330-1

Ziegler P.A., Schumacher M.E., Dèzes P., Van Wees J.-D. & Cloetingh S. 2006: Post-Variscan evolution of the lithosphere in the area of the European Cenozoic Rift System. In: Gee D.G. & Stephenson R.A. (Eds.): European Lithosphere Dynamics. *The Geological Society of London, Memoirs* 32, 97–112. https://doi.org/10.1144/GSL.MEM.2006.032.01.06

Electronic supplementary material is available online:
Fig. S1 at https://geologicacarpathica.com/data/files/supplements/GC-75-6-Mato-FigS1.jpg
Table S1 at https://geologicacarpathica.com/data/files/supplements/GC-75-6-Mato-TableS1.xlsx
Table S2 at https://geologicacarpathica.com/data/files/supplements/GC-75-6-Mato-TableS2.xlsx